Int. J. Multiphase Flow Vol. 10, No. 1, pp. 1–20, 1984
Printed in Great Britain.

0301–9322/84 $3.00 + .00
Pergamon/Elsevier

THE ANALYSIS OF PHASE SEPARATION PHENOMENA IN BRANCHING CONDUITS

NEMATOLLAH SABA and RICHARD T. LAHEY, JR.
Department of Nuclear Engineering, Rensselaer Polytechnic Institute, Troy, NY 12181, U.S.A.

(*Received* 15 *March* 1982; *in revised form* 13 *March* 1983)

Abstract—Phase separation phenomena in a two-phase (air/water) mixture flowing through a plexiglas tee test section was measured. It was found that even for low inlet flow qualities ($\leq 1\%$) the degree of phase separation was quite pronounced, with the gas phase preferentially separating into the branch. Using these data a physically-based empirical model was developed with which to calculate the phase distribution of a subsonic, two component, two-phase mixture in the downstream branches of a branching conduit. The model appears to correctly predict the observed phase separation in horizontal and vertical wyes and tees (having a horizontal branch). Moreover, although there is no data available for high pressure steam/water conditions, the predicted trends appear to be reasonable.

The model described in this paper is only considered to be valid for small conduits and mass withdrawal ratios (G_3A_3/G_1A_1) greater than 0.3.

1. INTRODUCTION

The analysis of light water nuclear reactor (LWR) loss-of-coolant accidents (LOCAs) requires that one be able to accurately calculate the two-phase flow splits in complex, branching conduits. The purpose of this paper is to present a general method for calculating phase separation in branching conduits.

A detailed search of the open literature disclosed that there are few experimental data and theoretical analyses on two-phase flow manifold distribution problems. The most important contributions are due to: Honan & Lahey (1981), Fouda (1974), Whalley & Azzopardi (1980), Henry (1981) and Collier (1975). Thus, an investigation was undertaken to provide a more thorough understanding of phase separation phenomena in branching conduits.

In particular, a detailed air/water experiment was performed in a tee test section to provide a data base for the development of an analytical model (Saba & Lahey 1982). The tee test section was designed and constructed from plexiglas, to allow for observation of the phenomena. It was installed (horizontally) in a large air/water loop at Rensselaer Polytechnic Institute (RPI). The data consisted of the various air and water inlet and outlet flows, the pressure gradients and the inlet pressure. In addition, flow visualization with high speed photography was performed.

Using the measured pressure gradients, the differential pressure at the tee junction was obtained by extrapolation. These data were used in the development of a physically-based empirical model for analysis of the phase distribution of a subsonic, two-component, two-phase mixture in the downstream branches of a branching conduit.

The resultant phase separation model is comprised to five conservation equations: The mixture conduity equation, the vapor-phase continuity equation, the mixture linear momentum equation for the branch, the mixture linear equation for the run, and the vapor-phase linear momentum equation for the branch. The simultaneous solution of these five equations provides the unknown parameters in the run and the branch of the tee.

2. DESCRIPTION OF TEST LOOP

The air/water loop, and tee test section, were used in an experiment which was designed to better understand phase separation phenomena in flowing two-phase mixtures. The test loop is shown schematically in figure 1.

The water in the test loop is stored in a collection tank from which it flows downward into the suction side of a centrifugal pump. After leaving the pump, part of the flow is

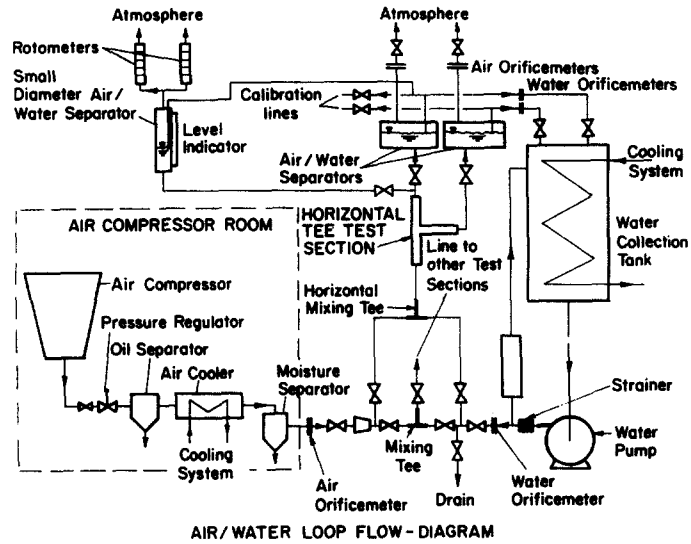

Figure 1. Air/water loop.

diverted through a filtering element and returned back to the collection tank. The remainder passes to a mixing tee, where it is combined with compressed air to achieve a two-phase flow.

The compressed air source is a positive displacement air compressor. After leaving the receiving tank, the compressed air passes through an oil separator, a pressure reducing valve, an after-cooler, a moisture separator and check valves. It then flows to the test section area and into the mixing tee.

From the mixing tee, the two-phase flow enters the test section in which the experiments were performed. The fluid exiting the test section is directed out through one, or both, parallel paths into air/water separation tanks. The water exits from the bottom of these tanks via two lines (one from each tank) which run parallel under the tanks, then up along the side of the water collection tank. The water is metered and then dumped into the collection tank, where it returns to atmospheric pressure. The air passes through a demister at the top of the separation tank, is metered, and then discharged outside the building.

The flows are controlled by a series of throttle valves. The inlet flow rates are controlled by two valves, upstream of the mixing tee on the air and water lines. The exit water flows are regulated by a valve on each of the water lines downstream of the separator tanks. In the same way, the air exiting the separator tanks is controlled by downstream valves.

The flows are measured by six calibrated flange-tap orifices. These are located upstream of the flow control valves previously described. The resulting orifice pressure differences are measured on U-tube manometers. The flows thus measured are the inlet air and water, and, exit air and water flow rates from both separator tanks.

Note in figure 1, that a small phase separation vessel with rotometers at the top, was also available. This small phase-separator was needed for cases in which we had a small air flow from the run of the tee.

The loop's piping system consisted of 3.81 cm diameter copper tubing. It was designed in such a way as to allow the different test sections in the loop to be interchanged with a minimum of changes in the plumbing, and no changes in valving or flow instrumentation. The test loop is rated for 0.7 MPa and air and water flow rates of 0.47 m^3/s and 4.42 kg/s, respectively.

3. TEST SECTION

The test section was a tee constructed from clear plexiglas. All legs of the tee had a inside diameter of 3.81 cm. The manufacturing process consisted of joining plexiglas pipe at the proper angle and then casting additional plexiglas around it, such that the resulting cross section was a 7.62 cm square. The machining and polishing process resulted in an optically clear section when viewed from any angle. The ends were then fitted with brass flanges to adapt the test section to the dopper pipe used in the loop.

Fourteen 1.6 mm pressure taps, 3.81 cm apart, were placed along the inlet, run and the branch piping of the tee test section. The test section was installed horizontally with the pressure taps at the bottom (to avoid air entrapment in the Δp lines). These pressure taps were used to measure the pressure gradient along the tee test-section. Tygon tubes from these pressure taps were lead to differential pressure transducers for reading the instantaneous differential pressure ($\Delta\tilde{p}$) along the tee test section.

The (electrical) output from the differential pressure transducers was time-averaged using a specially designed microprocessor. The length of time (T) used in the averaging process was chosen such that the resultant averaged pressure differential (Δp),

$$\Delta p(t) = \frac{1}{T}\int_{t-T}^{t} \Delta\tilde{p}(t')\,\mathrm{d}t',$$

was statistically stationary. For the conditions investigated in this study an averaging time (T) of 3 minutes was found to be sufficient.

The two-phase mixture entered the test section and flowed through it until it reached the branching junction. At this point, part of the flow continued straight along the pipe, while the other part was diverted out the branch. The water, having a much greater inertia, tended to go straight; whereas the apor (in our case, air) preferentially went into the branch, since it did not have enough inertia to overcome the adverse pressure gradient (i.e. pressure recovery) in the run. The result is that a much higher quality flow went into the branch than continued down the run.

4. EXPERIMENTAL MEASUREMENTS

For flow dividing at a tee junction there are two pressure changes which are of interest: the pressure loss experienced by the fluid flowing into the branch, and the pressure rise in the run. It should be noted that because we are dividing the flow at the tee junction, part of the pressure change is due to the Bernoulli effect.

For each experiment the desired flows were passed through the tee test section. The fluid exiting the branch and run of the test section was directed to the collecting tanks. The flow through each leg of the test section was controlled by the various inlet and outlet throttle valves. Hence the flow split could be varied as desired. Once a flow split was established, and the loop was completely stabilized, the various Δp were measured using the instrumentation shown in figure 2. The pressure gradients were then plotted in the manner shown in figure 3. The junction's pressure undershoot (for a case in which $w_3 = w_1$) in the branch, and recovery (for a case in which $w_3 < w_1$) in the run, is evident. Fortunately, the data was fully developed in the regions far upstream and downstream of the tee junction (i.e. the pressure gradient was due to wall frictiononly). Thus as shown schematically in figure 3, we were always able to extract (by extrapolation) the junction pressure differential (Δp_j).

The data taken are given in table 1. In all cases, side 1 is the entrance, side 2 is the run, and side 3 refers to the branch. Shown in this table are the: inlet mass flux; inlet flow quality; run flow quality; branch flow quality; flow fraction going through run; test section

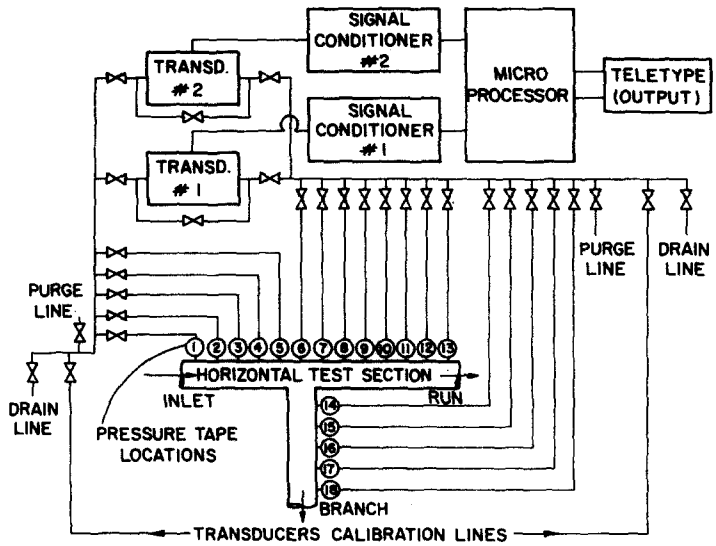

Figure 2. Tee test section-instrumentation schematic.

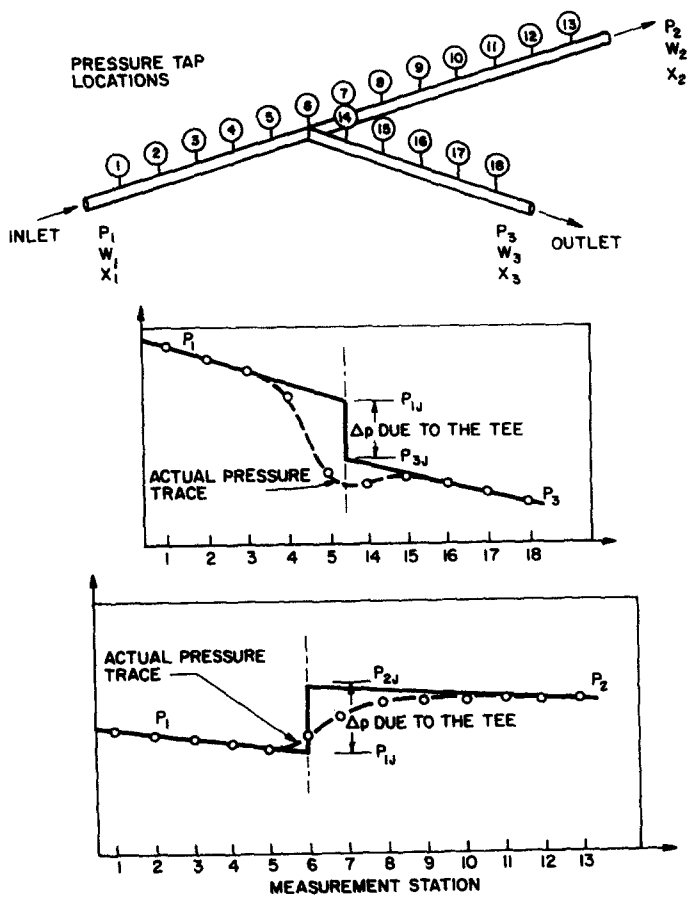

Figure 3. Typical pressure gradients in a tee.

Table 1. Phase separation data in a horizontal tee

Run	$G_1 \times 10^6$ (kg/hr-m^2)	x_1(%)	x_2(%)	x_3(%)	w_2/w_1	p_1 (kPa)	$(\Delta p_{1-3})_J$ (kPa)	$(\Delta p_{2-1})_J$ (kPa)	Flow Regime
1	4.88	0.00	0.0000	0.000	0.3	41.37	0.62	0.89	Single-Phase
2	4.88	0.00	0.0000	0.000	0.5	41.37	0.14	0.69	Single-Phase
3	4.88	0.00	0.0000	0.000	0.7	41.37	-	0.48	Single-Phase
4	4.88	0.10	0.0000	0.143	0.3	41.37	1.03	1.45	Stratified
5	4.88	0.10	0.0000	0.200	0.5	34.47	0.62	1.17	Stratified
6	4.88	0.10	0.0012	0.329	0.7	34.47	0.28	0.89	Stratified
7	4.88	0.25	0.0060	0.350	0.3	41.37	2.07	1.93	Stratified
8	4.88	0.25	0.0080	0.488	0.5	41.37	1.03	2.07	Stratified
9	4.88	0.25	0.0110	0.799	0.7	41.37	0.69	1.72	Stratified
10	4.88	0.50	0.0130	0.695	0.3	48.26	2.89	3.51	Stratified
11	4.88	0.50	0.0120	0.975	0.5	41.37	2.27	3.79	Wavy
12	4.88	0.50	0.0250	1.580	0.7	48.26	1.52	3.10	Stratified
13	4.88	1.00	0.0540	1.420	0.3	62.05	4.34	3.99	Slug
14	4.88	1.00	0.0650	1.960	0.5	48.26	3.10	4.27	Slug
15	4.88	1.00	0.0840	4.170	0.7	48.26	2.27	3.86	Slug
16	7.35	0.00	0.0000	0.000	0.3	55.15	1.39	1.45	Slug
17	7.35	0.00	0.0000	0.000	0.5	48.26	0.48	1.17	Single-Phase
18	7.35	0.00	0.0000	0.000	0.7	55.15	-	0.76	Single-Phase
19	7.35	0.10	0.0020	0.142	0.3	62.05	3.03	3.58	Wavy
20	7.35	0.10	0.0063	0.193	0.5	48.26	2.34	3.31	Wavy
21	7.35	0.10	0.0076	0.315	0.7	55.15	1.65	2.07	Wavy
22	7.35	0.25	0.0240	0.347	0.3	68.94	4.82	4.34	Slug
23	7.35	0.25	0.0240	0.476	0.5	41.37	3.10	4.89	Slug
24	7.35	0.25	0.0320	0.759	0.7	62.05	2.21	4.14	Slug
25	7.35	0.50	0.0780	0.687	0.3	48.26	7.03	5.93	Slug
26	7.35	0.50	0.085	0.924	0.5	41.37	5.51	6.20	Slug
27	7.35	0.50	0.091	0.470	0.7	48.26	3.30	5.65	Slug
28	7.35	1.00	0.166	1.380	0.3	48.26	9.99	9.24	Slug
29	7.35	1.00	0.158	1.870	0.5	55.15	7.24	10.61	Slug
30	7.35	1.00	0.160	2.850	0.7	55.15	4.41	8.82	Slug
31	9.76	0.00	0.000	0.000	0.3	55.15	2.07	2.27	Single-Phase
32	9.76	0.00	0.000	0.000	0.5	41.37	0.89	1.79	Single-Phase
33	9.76	0.00	0.000	0.000	0.7	55.15	0.14	1.24	Single-Phase
34	9.76	0.10	0.025	0.132	0.3	75.84	6.76	5.10	Slug
35	9.76	0.10	0.033	0.166	0.5	48.26	5.10	5.31	Slug
36	9.76	0.10	0.042	0.235	0.7	62.05	3.10	3.79	Slug
37	9.76	0.25	0.051	0.330	0.3	62.05	8.69	7.24	Slug
38	9.76	0.25	0.036	0.456	0.5	55.15	6.55	7.65	Slug
39	9.76	0.25	0.053	0.695	0.7	68.94	4.48	6.41	Slug
40	9.76	0.50	0.094	0.690	0.3	62.05	3.44	12.41	Slug
41	9.76	0.50	0.088	0.920	0.5	55.15	10.34	13.10	Slug
42	9.76	0.50	0.093	1.480	0.7	55.15	6.55	11.65	Slug
43	9.76	1.00	0.195	1.390	0.3	82.74	19.92	15.72	Slug
44	9.76	1.00	0.211	1.720	0.5	55.15	13.65	18.13	Slug
45	9.76	1.00	0.250	2.590	0.7	68.94	7.65	14.13	Slug

inlet pressures; extrapolated junction pressure drop from inlet-to-branch; extrapolated junction pressure recovery from inlet-to-run; and, the observed flow regime.

5. PHASE SEPARATION MODEL DEVELOPMENT

A phase separation model was developed using the appropriate two-phase conservation equations. This model can be used to calculate the phase distribution of a subsonic, two-component, two-phase mixture in a branching conduit. The model predicts that the two phases may separate unevenly into the downstream branches.

In a typical branching conduit (wye or tee), such as the tee shown schematically in figure 3, there are eight parameters of interest: x_1, $\Delta p_{1\text{-}3}$, $\Delta p_{1\text{-}2}$, G_1, G_2, G_3, x_2, x_3. To have a well-posed problem we can specify three (3) of these parameters (e.g. x_1, G_1 and $\Delta p_{1\text{-}3}$, or, x_1, $\Delta p_{1\text{-}3}$ and $\Delta p_{1\text{-}2}$). The remaining five parameters can then be considered to be the dependent variable (i.e. unknowns) of the problem. This requires us to have five independent conservation laws. The conservation equations used were: the mixture continuity equation, the vapor-phase continuity equation, the mixture linear momentum equation for the branching flow, the mixture linear momentum equation for flow in the run, and the vapor-phase linear momentum equation for the branching flow. We will now consider these equations one at a time.

The mixture continuity equation

$$G_1 A_1 = G_2 A_2 + G_3 A_3 \tag{1}$$

where the subscripts 1, 2 and 3 refer to the fully developed conditions at the inlet, run, and the side branch sections, respectively.

The vapor phase continuity equation

$$G_1 x_1 A_1 = G_2 x_2 A_2 + G_3 x_3 A_3 . \tag{2}$$

In order to further describe the flow split, we need two mixture linear momentum equations; one for the branching flow, and the other for the run. These two mixture momentum equations are used to quantify the pressure change across the branching junction.

The mixture linear momentum equation for the branch

$$\Delta p_{1\text{-}3} \triangleq p_1 - p_3 = p_1 - p_{1J} + (\Delta p_{1\text{-}3})_J + p_{3J} - p_3 \tag{3}$$

where, $p_1 - p_{1J}$, represents the pressure loss in the inlet section; $(\Delta p_{1\text{-}3})_J$, represents the pressure loss in the junction due to the turning of the fluid into a side branch; and $p_{3J} - p_3$, represents the pressure loss in the side branch, downstream of the junction (J).

We know that $(\Delta p_{1\text{-}3})_J = p_{1J} - p_{3J}$ represents both the reversible and irreversible pressure changes, while the pressure losses in the inlet and side branch sections are only due to wall shear and gravity effects. The three components of pressure loss from station 1 to station 3 are given by the following equations:

$$p_1 - p_{1J} = \frac{K_1}{2g_c}\frac{G_1^2}{\rho_L}\phi^2_{Lo_1} + \bar{\rho}_1 \frac{g}{g_c} L_1 \sin \gamma_1 \tag{4}$$

$$p_{3J} - p_3 = \frac{K_3}{2g_c}\frac{G_3^2}{\rho_L}\phi^2_{Lo_3} + \bar{\rho}_3 \frac{g}{g_c} L_3 \sin \gamma_3 \tag{5}$$

where, $K_i \triangleq f_i L_i / D_{H_i}$; f_i, if the Darcy–Weisbach friction factor; L_i, is the length of section-i ($i = 1, 3$); ϕ^2_{Lo}, is the two-phase multiplier in section-i; γ_i, is the angle of inclination from the horizontal in section i; D_{H_i}, is the hydraulic diameter of section i; and $\bar{\rho}_i$ is the two-phase density in section i.

In this study it was found to be sufficient to use a homogenous multiplier in the various

sections, thus,

$$\phi_{Lo_i}^2 = \left(1 + \frac{v_{LG}}{v_L} x_i\right) \qquad [6]$$

where,

$$v_{LG} = \left(\frac{1}{\rho_G} - \frac{1}{\rho_L}\right) = \frac{(\rho_L - \rho_G)}{\rho_G \rho_L}.$$

The junction pressure differential, $(\Delta p_{1\text{-}3})_J$, can be partitioned into a reversible and irreversible part,

$$(\Delta p_{1\text{-}3})_J = (\Delta p_{1\text{-}3})_{\text{REV}} + (\Delta p_{1\text{-}3})_{\text{REV}}. \qquad [7]$$

Now, the so-called Chisholm local loss two-phase multiplier ($\Phi = \rho_L/\rho'$) can be written as,

$$\Phi = (1 - x_1)^2 \left[1 + \frac{C_{1\text{-}3}}{X_{tt}} + \frac{1}{X_{tt}^2}\right]. \qquad [8]$$

Thus,

$$(\Delta p_{1\text{-}3})_{\text{IRREV}} = \frac{K_{1\text{-}3}}{2g_c} \frac{G_1^2}{\rho_L} (1 - x_1)^2 \left[1 + \frac{C_{1\text{-}3}}{X_{tt}} + \frac{1}{X_{tt}^2}\right] \qquad [9]$$

where for sufficiently high Reynolds numbers,

$$\frac{1}{X_{tt}} = \left(\frac{x_1}{1 - x_1}\right)\left(\frac{\rho_L}{\rho_G}\right)^{1/2},$$

and, $K_{1\text{-}3}$ is the single-phase loss coefficient for the tee junction, given by Saba & Lahey (1982) as,

$$K_{13} = \left[1.18 + \left(\frac{G_3 A_3}{G_1 A_1}\right)^2 - 0.8\left(\frac{G_3 A_3}{G_1 A_1}\right)\right]\left(\frac{A_1}{A_3}\right). \qquad [10]$$

The general form of $C_{1\text{-}3}$ is (Chisholm 1967),

$$C_{1\text{-}3} = \left[1 + (C_3 - 1)\left(\frac{\rho_L \rho_G}{\rho_L}\right)^{1/2}\right]\left[\left(\frac{\rho_L}{\rho_G}\right)^{1/2} + \left(\frac{\rho_G}{\rho_L}\right)^{1/2}\right]. \qquad [11]$$

For slip flow conditions, the suggested value for C_3 is 1.75. For homogeneous flow, $C_3 = 1.0$, and [11] becomes,

$$C_{1\text{-}3} = \left[\left(\frac{\rho_L}{\rho_G}\right)^{1/2} + \left(\frac{\rho_G}{\rho_L}\right)^{1/2}\right]. \qquad [12]$$

The reversible pressure change is given by the two-phase Bernoulli equation, written in the form (Saba & Lahey 1982),

$$(\Delta p_{1\text{-}3})_{\text{REV}} = \frac{\rho_{H_3}}{2g_c}\left[\frac{G_3^2}{(\rho_3'')^2} - \frac{G_1^2}{(\rho_1'')^2}\right] \qquad [13]$$

where the so-called energy (ρ''') and homogenous (ρ_H) densities (Lahey & Moody 1977) are given by,

$$\frac{1}{(\rho_i''')^2} \triangleq \left[\frac{(1-x_i)^3}{\rho_L^2(1-\alpha_i)^2} + \frac{x_i^3}{\rho_G^2\alpha_i^2}\right] \quad [14]$$

and,

$$\rho_{H_3} = \frac{1}{(v_L + x_3 v_{LG})}. \quad [15]$$

The mixture linear momentum equation for the run

In a similar manner, the pressure change between the inlet and the run can be assumed to be made up of three components: that due to the inlet section, the junction, and the downstream section. Specifically,

$$\Delta p_{1\text{-}2} \triangleq p_1 - p_2 = (p_1 - p_{1J}) + (\Delta p_{1\text{-}2})_J + (p_{2J} - p_2) \quad [16]$$

where, as before,

$$p_1 - p_{1J} = \frac{K_1}{2g_c}\frac{G_1^2}{\rho_L}\phi_{Lo_1}^2 + \bar{\rho}_1\frac{g}{g_c}L_1 \sin\gamma_1, \quad [17]$$

$$p_{2J} - p_2 = \frac{K_2}{2g_c}\frac{G_2^2}{\rho_L}\phi_{Lo_2}^2 + \bar{\rho}_2\frac{g}{g_c}L_2 \sin\gamma_2 \quad [18]$$

and,

$$(\Delta p_{1\text{-}2})_J = p_{1J} - p_{2J} = \frac{K_{1\text{-}2}}{2g_c}\left[\frac{G_2^2}{\rho_2'} - \frac{G_1^2}{\rho_1'}\right] = -(\Delta p_{2-1})_J \quad [19]$$

Here, K_{1-2} is an empirical pressure recovery coefficient which was determined from the single-phase data reported in table 1 (Saba & Lahey 1982),

$$K_{1\text{-}2} = 0.11 + \frac{5.0}{\left[\frac{G_1 D_{H_1}}{\mu_{L_1}}\right]^{0.17}} \quad [20]$$

and ρ', the so-called momentum density (Lahey & Moody 1977), is given by,

$$\frac{1}{\rho_i'} \triangleq \left[\frac{(1-x_i)^2}{\rho_L(1-\alpha_i)} + \frac{x_i^2}{\rho_g\alpha_i}\right]. \quad [21]$$

So far we have only four independent conservation equations; the extra equation needed for closure of the problem is the vapor-phase linear momentum equations for the branch.

The vapor-phase linear momentum equation for the branch

The steady vapor-phase linear momentum equation along the branching stream lines, for the situation in which there is no phase change, is given by (Saba & Lahey 1982),

$$-\alpha\frac{dp}{dz} = \alpha F_d + \frac{1}{g_c}\alpha\rho_G u_G\frac{du_G}{dz} + \alpha F_w + \frac{g}{g_c}\rho_G\alpha \sin\gamma_{1\text{-}3} \quad [22]$$

where, u_G is the gas phase valocity, F_d is the volumetric interfacial drag force on the vapor, and, F_w is the volumetric wall drag force on the vapor in the junction. Integration [22] along the vapor streamlines through the junction we obtain (Saba & Lahey 1982),

$$(\Delta p_{1\text{-}3})_J = \frac{3}{4}\frac{\rho_L}{g_c}\left(\frac{C_D}{D_B}\right)U_{r_J}^2 + \frac{\rho_{G_3}}{2g_c}\left[\frac{(G_3x_3)^2}{(\rho_{G_3})^2\alpha_3^2} - \frac{(G_1x_1)^2}{(\rho_{G_1})^2\alpha_1^2}\right] + \frac{K_{1\text{-}3}}{2g_c}\frac{(G_1x_1)^2}{\rho_{G_1}\alpha_1^2} + \frac{g}{g_c}\rho_{G_3}L_J\sin\bar{\gamma}_{1\text{-}3}. \quad [23]$$

For the case of interest in this study, a horizontal tee, $\bar{\gamma}_{1\text{-}3} = 0$.

The reason for integrating along a vapor streamline which enters into the side branch, rather than following one that continues into the run, is that the ability of the vapor to make the turn into the side branch is the dominant factor which affects the phase distribution of two-phase mixtures. Thus transverse momentum conservation on the vapor was considered to be the most important effect to be modelled. Figure 4 shows the pronounced phase separation observed in a typical run. It can be seen that some of the vapor actually overshoots the junction, then moves against the mean flow into the branch.

In [23], the parameter (C_D/D_B) is the cross sectionally averaged one-dimensional drag coefficient (having dimensions of reciprocal length). This parameter is a function of α, the cross-sectionally averaged void fraction.

In this study we have assumed the validity of Hench's (churn-turbulent) drag model (Hench & Johnston 1968),

$$\left(\frac{C_D}{D_B}\right) = 54.9\left[\frac{\rho_G}{\rho_L}\alpha(1-\alpha)^2 + (1-\alpha)^3\right], \quad (\mathrm{m}^{-1}) \quad [24]$$

Note, for low pressure air/water flows, $\rho_G \ll \rho_L$, thus [26] becomes,

$$(C_D/D_b) = 54.9(1-\alpha)^3, \quad (\mathrm{m}^{-1}). \quad [25]$$

The length L_J in [23] can be viewed as an equivalent path length of the mean vapor streamline. It has been correlated using the two-phase data in table 1 (Saba & Lahey 1982),

$$L_J = 2.81D_{H_3}\left[e^{-0.12}\left(\frac{1-x_1}{x_1}\right)^{0.15}\left(\frac{\rho_{G_1}}{\rho_{L_1}}\right)^{1/2}\right]\left[\left(\frac{G_3}{G_1}\right)^{(1-x_1)^3}\right][(1-x_3)^3]. \quad [26]$$

The void fraction and relative velocity were determined from the standard Zuber–Findlay drift-flux relation (Lahey & Moody 1977),

$$\alpha_i = \frac{x_i}{C_0\left[x_i + \frac{\rho_{G_i}}{\rho_{L_i}}(1-x_i)\right] + \frac{\rho_{G_i}V_{Gj_i}}{G_i}} \quad [27]$$

and,

$$U_{r_i} \triangleq u_{G_i} - u_{L_i} = \frac{j_i(C_0-1) + V_{Gj_i}}{(1-\alpha_i)} \quad [28]$$

where, the volumetric flux is given by,

$$j_i \triangleq G_i\left[\frac{x_i}{\rho_{G_i}} + \frac{(1-x_i)}{\rho_{L_i}}\right] \quad [29]$$

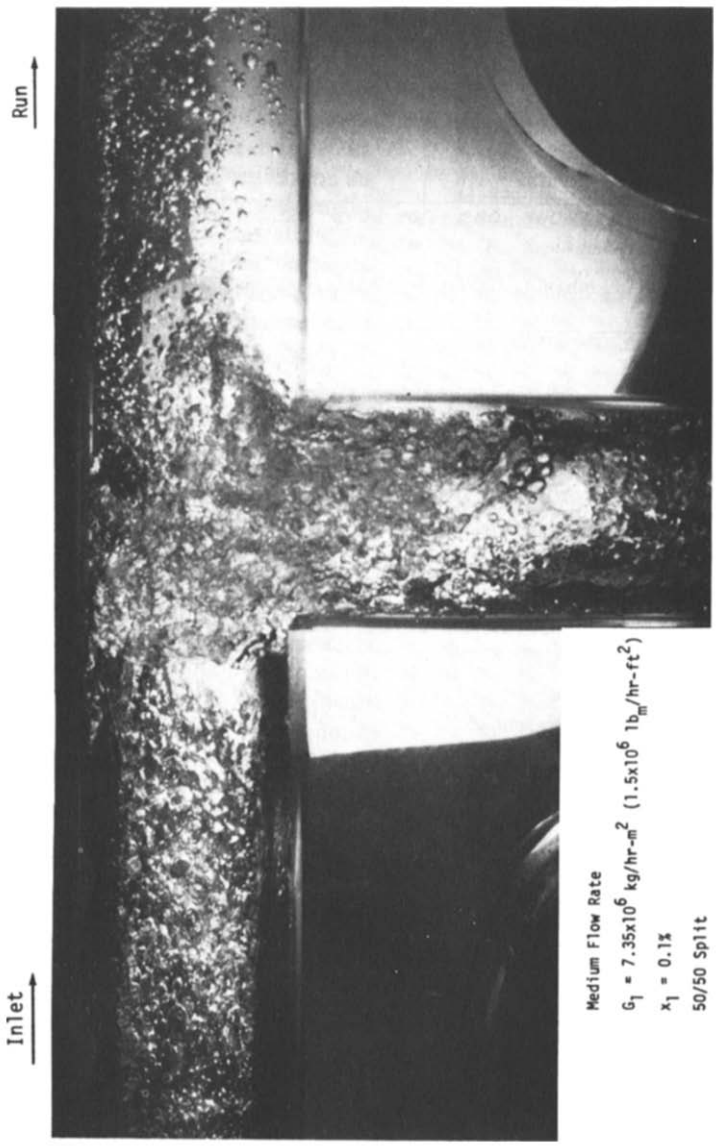

Figure 4. Top view of horizontal tee.

Concentration parameter, C_o, is defined (Lahey & Moody 1977) as,

$$C_0 \triangleq \int_{A_{x-s}} \int j\alpha \, da \Big/ \left[\left(\int_{A_{x-s}} \int j \, da \right) \left(\int_{A_{x-s}} \int \alpha \, da \right) \right] \qquad [30]$$

the appropriate value of C_0 at the junction was found to be, (Saba & Lahey 1982),

$$C_{0_J} = 1.4 - 0.4 \left(\frac{\rho_{G_1}}{\rho_{L_1}} \right)^{1/2} \qquad [31]$$

The drift-velocity, V_{Gj}, is defined (Lahey & Moody 1977) as,

$$V_{Gj} \triangleq \int_{A_{x-s}} \int \alpha (u_G - j) \, da \Big/ \int_{A_{x-s}} \int \alpha \, da. \qquad [32]$$

For bubbly and churn-turbulent flows we can use (Lahey & Moody 1977),

$$V_{Gj} = k_3 \left[\frac{(\rho_{L_1} - \rho_{G_1})\sigma}{\rho_1^2} g g_c \right]^{1/4} \sin \bar{\theta}_{1-3} \qquad [33]$$

where it is frequently assumed that $k_3 = 2.5$ (Lahey & Moody 1977). It should be noted that for the case of interest here $\bar{\theta}_{1-3} = 0$, thus the choice of the parameter k_3 is of no significance.

Equations[1]–[33] comprise the phase separation model. These equations can be solved in a variety of ways (Saba & Lahey 1982), for virtually any choice of well-posed boundary conditions.

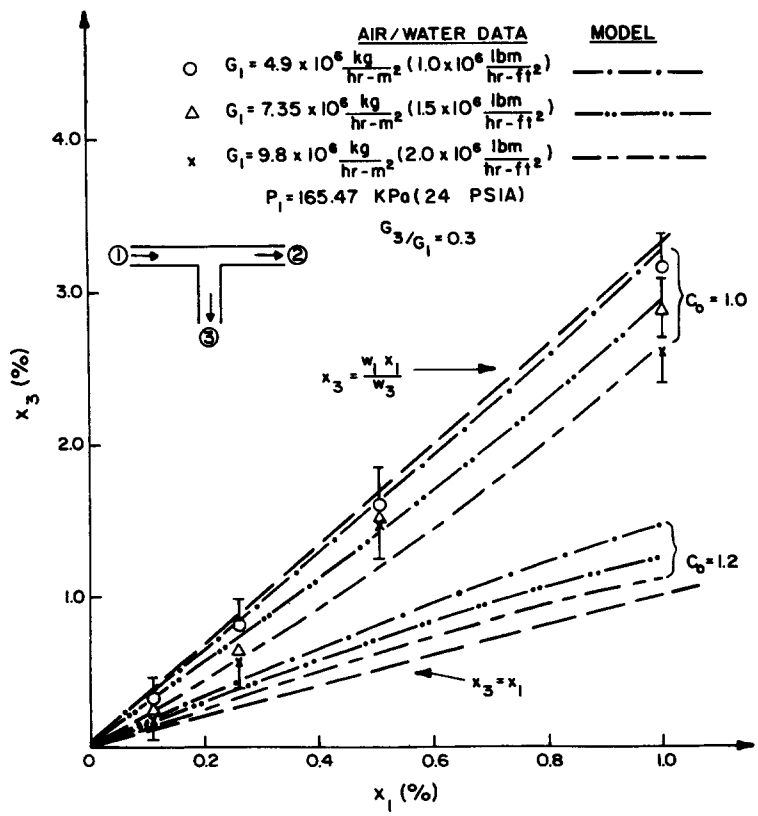

Figure 5. Comparison of air/water predicted branch quality with experimental data: $G_3/G_1 = 0.3$.

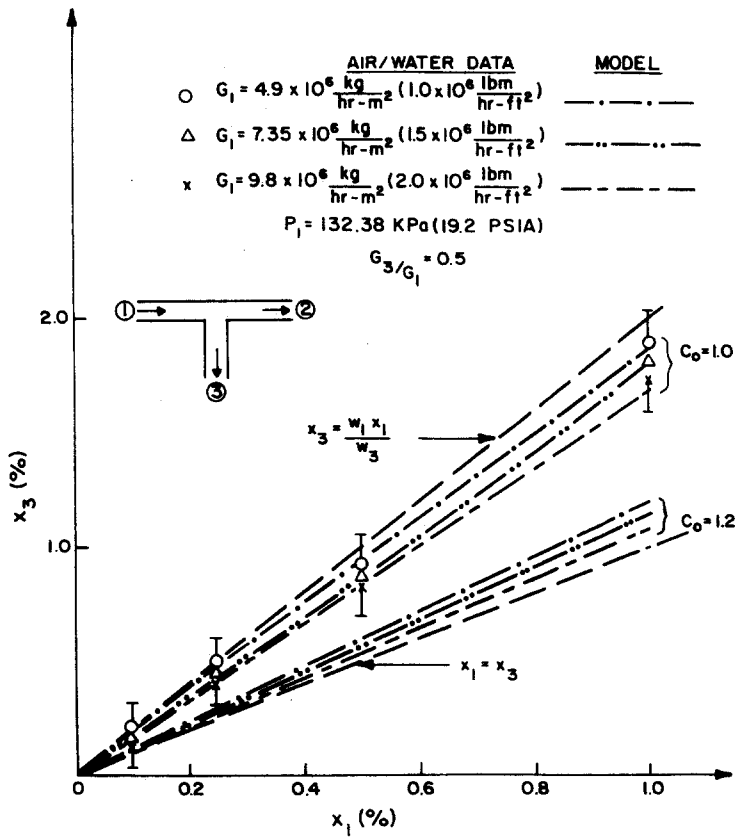

Figure 6. Comparison of air/water predicted branch quality with experimental data: $G_3/G_1 = 0.5$.

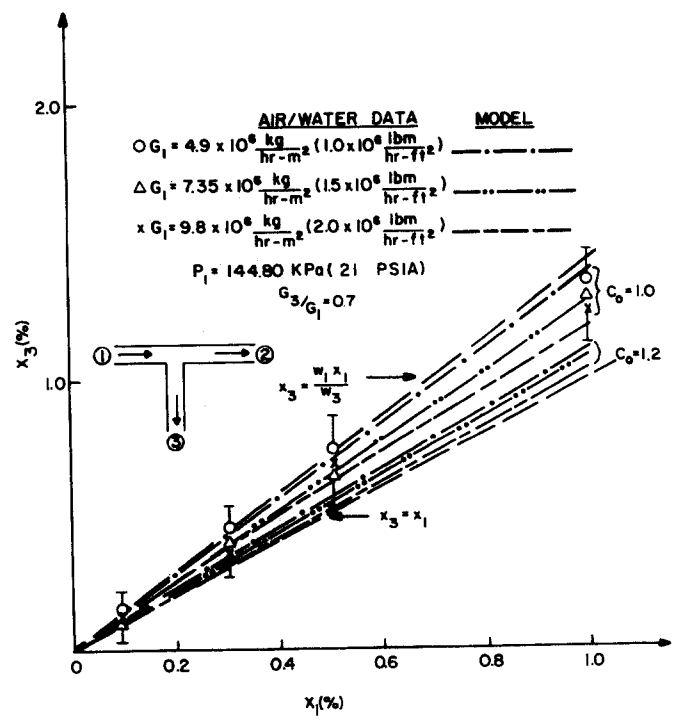

Figure 7. Comparison of air/water predicted branch quality with experimental data: $G_3/G_1 = 0.7$.

6. MODEL PREDICTION CAPABILITY

The following will be a discussion of the results of the phase separation model which was evaluated using the same boundary conditions as the measured air/water data, and for hypothetical steam/water conditions.

Figures 5–7 compare the predicted flow quality (x_3) with the corresponding data. It can be seen that the agreement is within the data uncertainty intervals for the assumption of homogenous flow ($C_0 = 1.0$) in the various legs of the branching conduit.

It should be noted that both the data and model predictions are much closer to the line of total vapor phase separation ($x_3 = w_1 x_1 / w_3$) than it is to the line of equal phase separation ($x_3 = x_1$). This is significant, since it has been standard practice in the past analyses to assume equal phase separation in branching conduits.

The data presented in figure 8 summarizes the data trends of previous RPI air/water phase separation data (Honan & Lahey 1981), taken in vertical wye and tee test section. It can be seen that the data trends are very similar to those in figures 5–7. Since the degree of phase separation shown in figure 8 was round to be insensitive to the angle of the branch (θ), it appears that the phase separation model reported herein may be used for the prediction of phase separation in branching conduits other than tees.

Figures 9–11 are plots of predicted and measured $(\Delta p_{1\text{-}3})_J$ at the junction of the tee test section, and figures 12–14 are the corresponding plots of $(\Delta p_{2\text{-}1})_J$. The agreement between the data and the homogeneous model ($C_0 = 1.0$) is seen to be quite good.

It should be noted that all the RIP data has been taken at low inlet flow qualities (x_1). The phase separation model presented in section 5 has been based on these data. Nevertheless, as can be seen in figures 15 and 16, when this model is compared with other data (Collier 1975), which was tekan at higher inlet qualities, the agreement is again seen to be quite good. It is interesting to note, however, that the best agreement is achieved for slip flow conditions ($C_0 = 1.2$). This is apparently due to the fact that these data were taken for a different flow regime (annular) than our data. For annular flow, Hench's (1968), churn-turbulent interfacial drag model, [26], is no longer valid. Moreover, the branch loss coefficient, $K_{1\text{-}3}$, which was used to predict the values shown in figures 15 and 16, was taken from our data [10], and islikely not appropriate. Fortunately, the overall predictions of branch flow quality (x_3) do not appear to be too sensitive to these distortions.

While no steam/water wye or tee phase separation data has been reported in the literature, it is interesting to evaluate the pressure effect implicit in the model. This was done for the geometry of the RPI test section. It can be seen in figure 17 that the pressure effect is reasonable and goes to the right limit (i.e. $x_3 = x_1$) at the critical pressure (p_c). Even though there is no steam/water data currently available with which to assess our model, it is comforting to see that the model has the correct asymptotic behavior.

If the quality range of this hypothetical steam/water experiment is extended, as shown in figure 18, we see that after a certain inlet quality (x_1), the model predicts $x_3 = 100\%$. Since these conditions are well outside the range of data that the current model was based on, it is not known if this prediction is valid.

7. SUMMARY AND CONCLUSIONS

A complete set of phase separation data has been taken in a horizontal tee. These data are consistent with previous data (Honan & Lahey 1981) taken in vertical wyes and tees. The degree of phase separation seen in these data is quite pronounced, with the gas phase preferentially separating into the branch.

A physically-based empirical phase separation model has been developed. This model appears to correctly predict the observed phase separation in branching conduits for well mixed, subsonic, flow regimes. It can be anticipated, however, that the model may yield

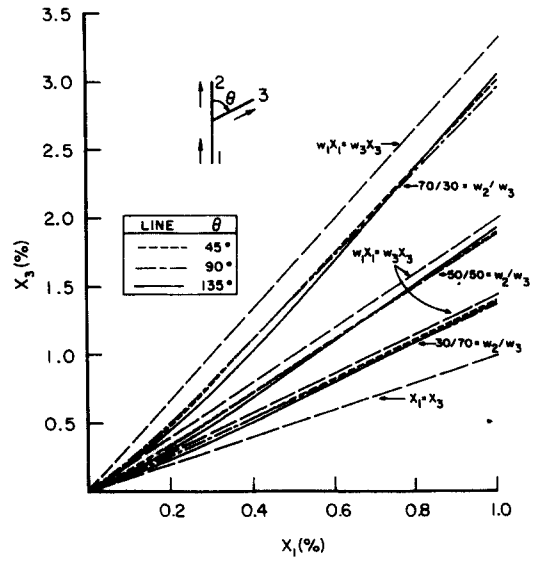

Figure 8. x_3 vs x_1, combined RPI branch quality data; vertical wyes and tees (Honon & Lahey 1981).

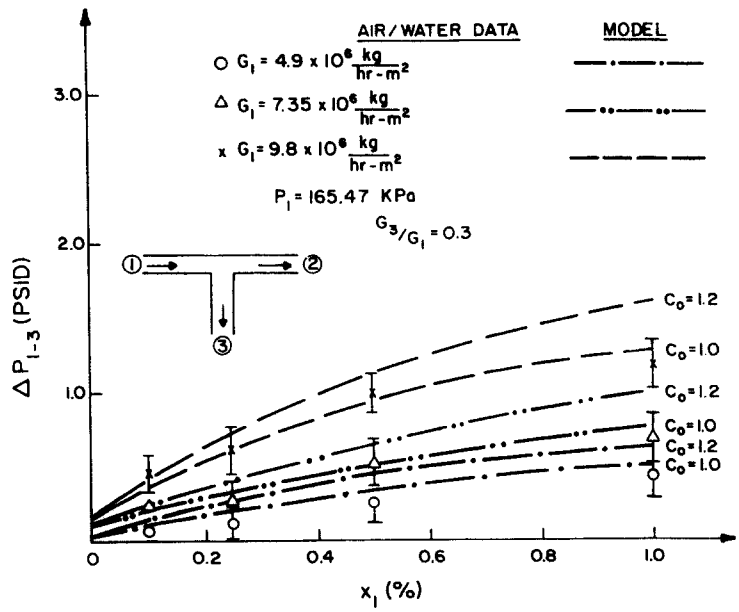

Figure 9. Comparison of air/water predicted branch pressure drop with experimental data: $G_3/G_1 = 0.3$.

incorrect results for stratified flow regimes in which the branch is vertical. Subsequent to liquid entrainment (for a top branch) or vapor pull-through (for a bottom branch), the model may yield reasonable results; however further data is required to quantify this hypothesis.

For most cases of one-component two-phase flows, the model is also expected to be fairly accurate since flashing (in the branch) and condensation (in the run) effects are not normally too large. Clearly, however, to fully generalize the model, more data are needed

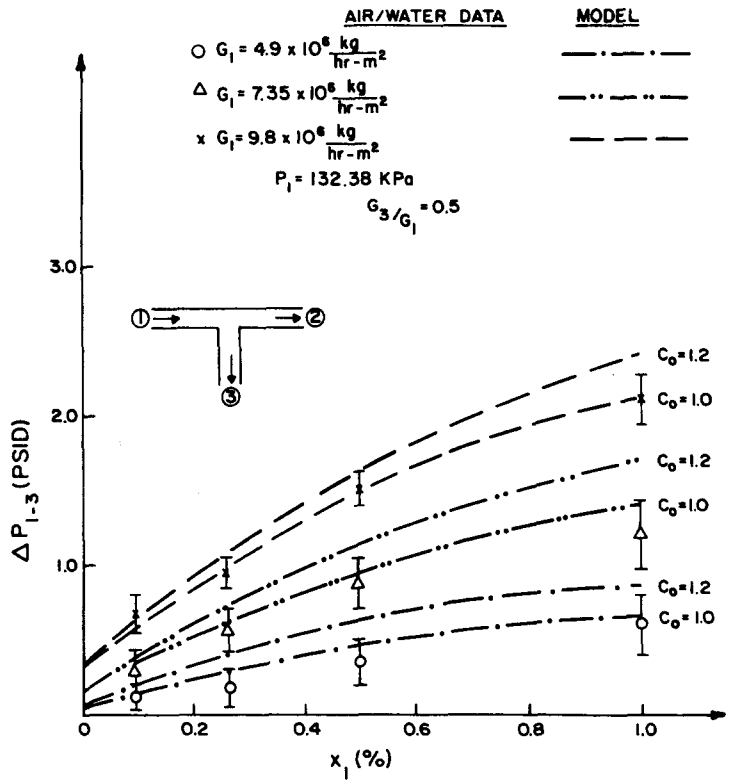

Figure 10. Comparison of air/water predicted branch pressure drop with experimental data: $G_3/G_1 = 0.5$.

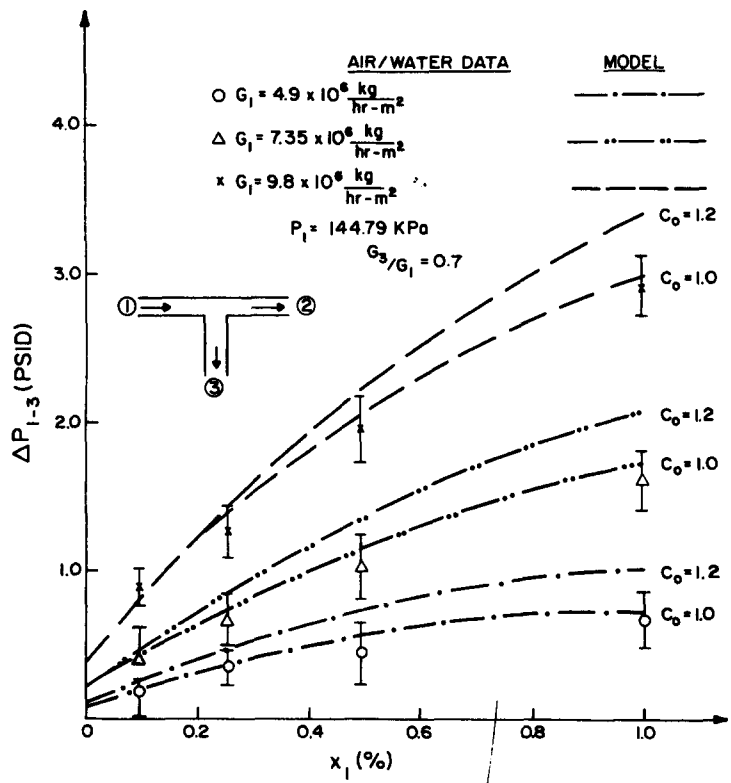

Figure 11. Comparison of air/water predicted branch pressure drop with experimental data: $G_3/G_1 = 0.7$.

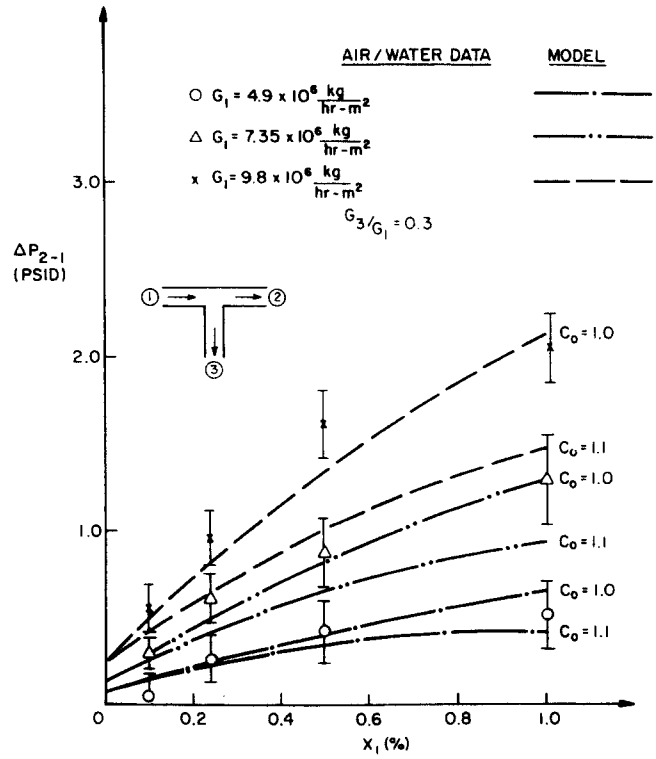

Figure 12. Comparison of air/water predicted run pressure recovery with experimental data: $G_3/G_1 = 0.3$.

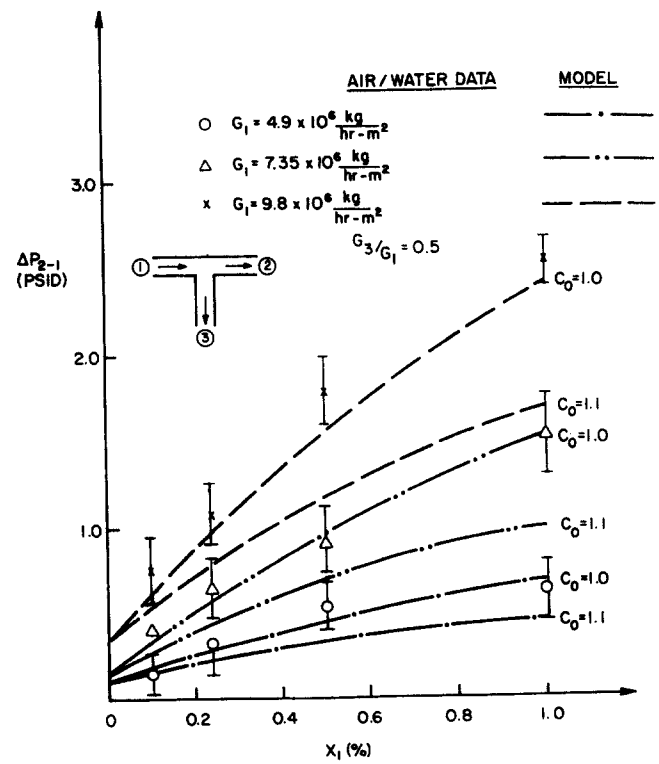

Figure 13. Comparison of air/water predicted run pressure recovery with experimental data: $G_3/G_1 = 0.5$.

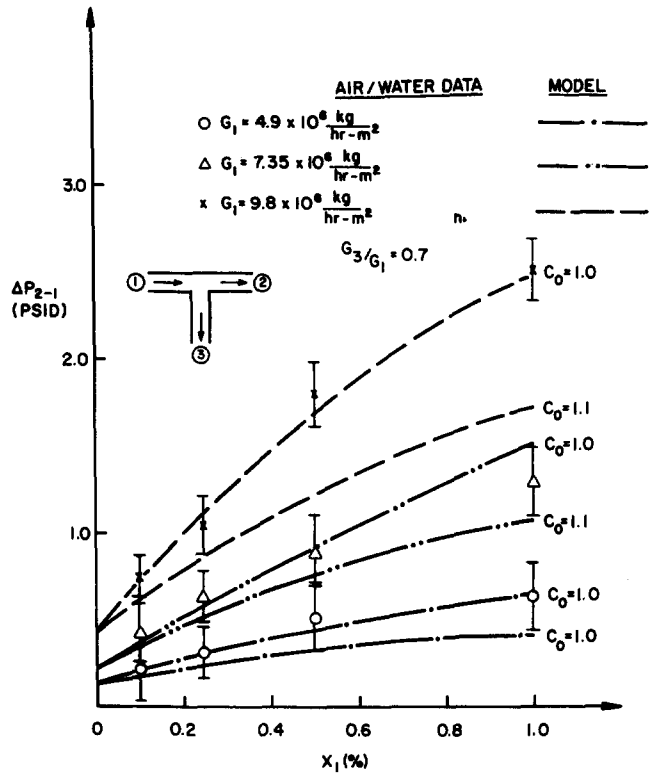

Figure 14. Comparison of air/water predicted run pressure recovery with experimental data: $G_3/G_1 = 0.7$.

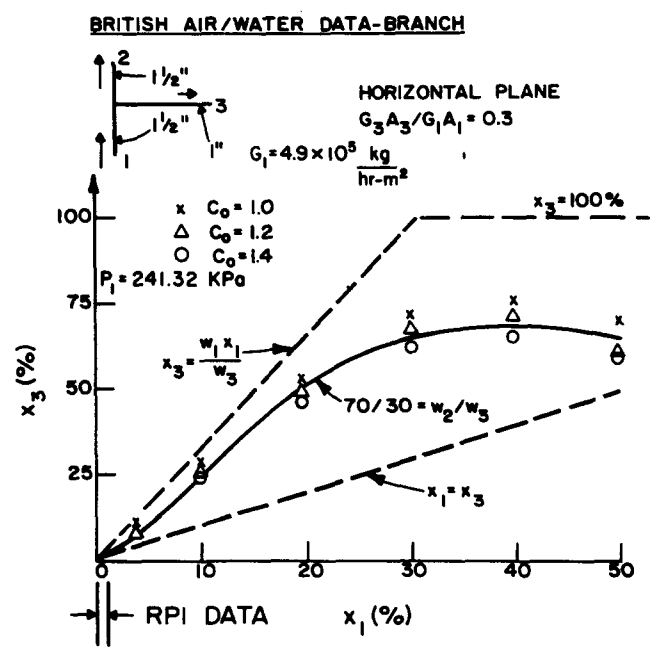

Figure 15. Comparison of air/water predicted branch quality with british data (Collier 1975): $G_3/G_1 = 0.3$.

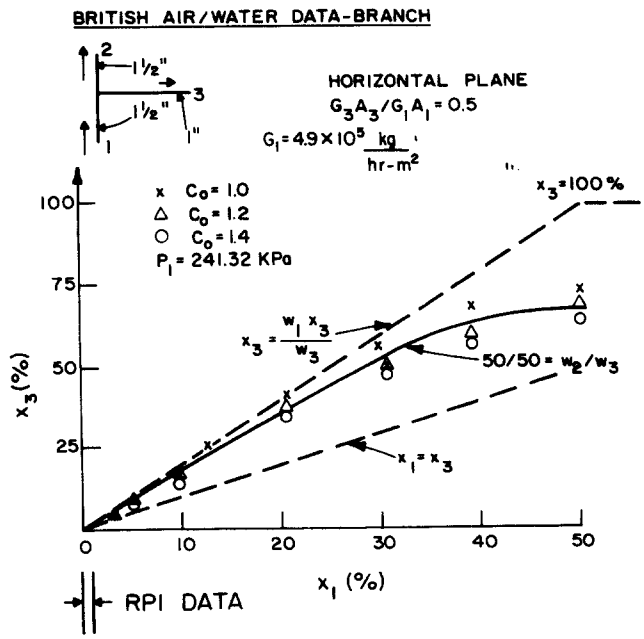

Figure 16. Comparison of air/water predicted branch quality with British data (Collier 1975): $G_3/G_1 = 0.5$.

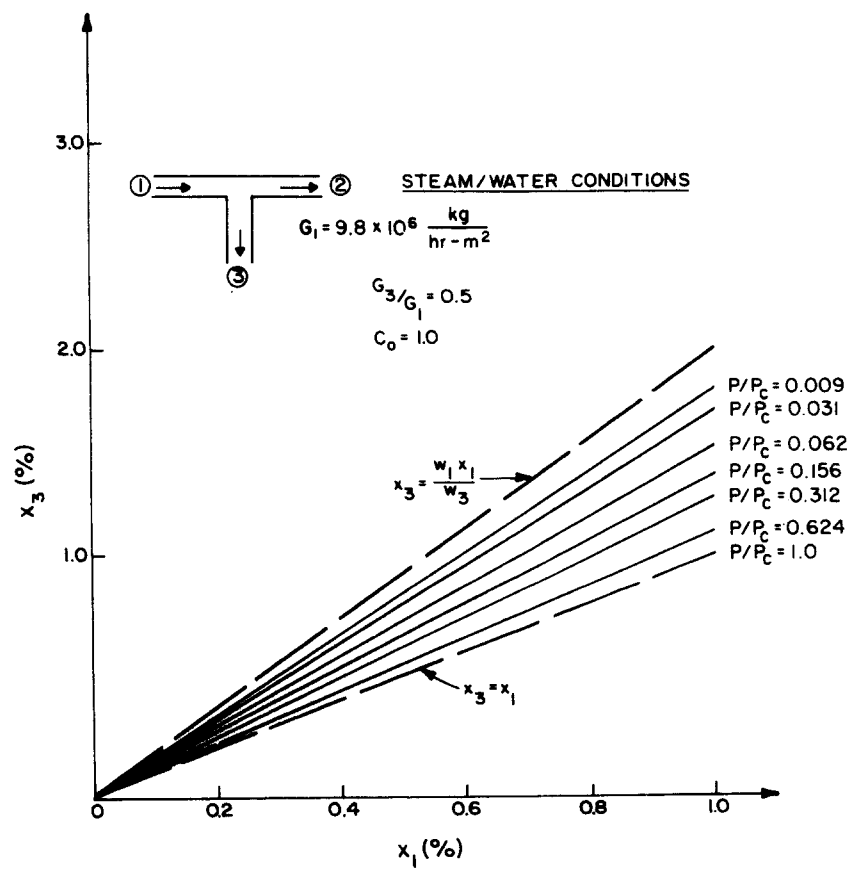

Figure 17. Predicted steam/water branch quality for various pressures.

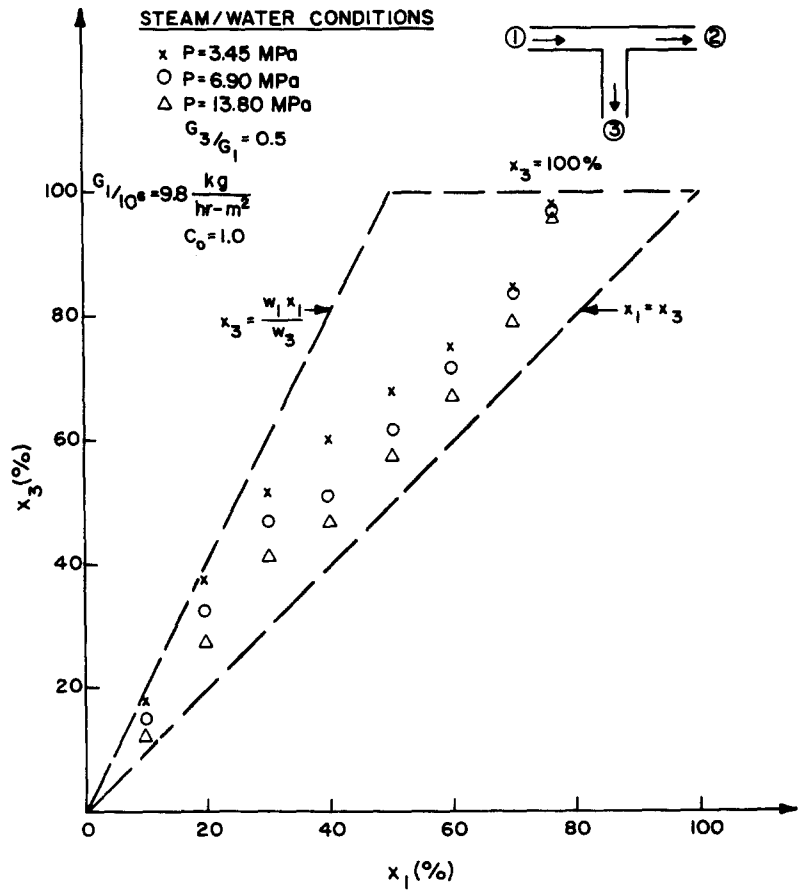

Figure 18. Predicted steam/water branch quality for high inlet qualities.

in different geometric configurators, at higher inlet qualities (x_1), with different fluids, (e.g. steam/water) and at higher system pressures. It is hoped that this paper will stimulate other investigators to perform such experiments.

Acknowledgements—The authors gratefully acknowledge the financial support given this study by the USNRC, and the stimulating technical discussions with Professor D. A. Drew (RPI) and Mr. L. Cheng (RPI).

NOMENCLATURE

A_{x-s} cross-section flow area
C_0 void concentration parameter in the conduits
C_{0_J} void concentration parameter in the junction
D_H $4A_{x-s}/P_f$, hydraulic diameter
f Darcy–Weisbach friction factor
F force
G mass flux
g gravitational acceleration
j_G volumetric flux of vapor phase
j_L volumetric flux of liquid phase
K hydraulic loss coefficient
L_J vapor path length in junction
p static pressure
P_f friction perimeter

S slip ratio
u_k valocity of phase, k
U_r one-dimensional averaged relative velocity
V_{Gj} drift velocity
w_i flow rate in conduit, i
x_i flow quality in conduit, i
X_{tt} Martinelli parameter
α void fraction
γ_i angle of inclination from the horizontal of section i
ρ density
ρ_H homogeneous (i.e. no-slip) density
ρ' momentum density
ρ''' energy density
σ surface tension
ϕ branching angle
ϕ^2_{Lo} two-phase friction loss multiplier
Φ two-phase local loss multiplier
μ_L liquid phase viscosity

Subscripts

d drag
J junction
L liquid phase
LG difference between vapor and liquid properties
G vapor phase
w wall
I inlet
2 run
3 branch
1θ single-phase
2ϕ two-phase

REFERENCES

CHISHOLM, D. 1973 Pressure gradients due to friction during the flow of evaporating two-phase mixtures in smooth tubes and channels. *Int. J. Heat Mass Transfer* **16**, 347–358.

CHISHOLM, D. 1967 Pressure loss in bends and tees during steam/water flow. NEL Report No. 318.

COLLIER, J. G. 1975 Single-phase and two-phase behavior in primary circuit components. Symposium on Two-Phase Flow and Heat Transfer in Water-Cooled Nuclear Reactors, Dartmouth University, 4–8 August.

FOUDA, A. E. & RHODES, E. 1974 Two-phase annular flow stream division in a simple tee. *Trans. Inst. Chem. Engrs* **52**, 354–360.

HENCH, J. E. & JOHNSTON, J. P. 1968 Two-dimensional diffuser performance with subsonic two-phase air/water flow, APED-5477.

HENRY, J. A. R. 1981 Dividing annular flow in a horizontal tee. *Int. J. Multiphase Flow* **7**, 343–355.

HONAN, T. J. & LAHEY, R. T. JR. 1981 The measurement of phase separation in wyes and tees. *Nucl. Engng Design* **64**, 93–102.

LAHEY, R. T. JR. & MOODY, F. J. 1977 The thermal-hydraulics of a boiling water nuclear reactor. ANS Monograph.

SABA, N. & LAHEY, R. T. JR. 1982 Phase separation phenomena in branching conduits. NUREG/CR-2590.

WHALLEY P. B. & AZZOPARDI, B. J. 1980 Two-phase flow in a tee junction. AERE-R 9699.